 DOI: 10.1086/682276

Appendix from A. W. Bateman et al., "Generational Spreading Speed and the Dynamics of Population Range Expansion" (Am. Nat., vol. 186, no. 3, p. 000)

Mathematical Details

Mathematical Background

IDE Models of Invasion

Consider a discrete-time model for growth of a demographically unstructured population in continuous space:

$$n(y, t+1) = b_n(y)n(y, t), \tag{A1}$$

where $n(y, t)$ represents population density at location y ($\in \mathbb{R}$) and time step t ($\in \mathbb{N}$) and b_n is the associated density-dependent per capita population growth rate.

To describe the population's movement in space, we can use a dispersal kernel, $k(x, y)$, giving the probability density with which individuals at location y move to location x in a single time step. Assuming that the environment is spatially homogeneous (Kot et al. 1996; Neubert and Caswell 2000), b_n depends only on population density and k depends only on the relative positions of x and y, so $b_n(y)$ becomes b_n and $k(x, y)$ becomes $k(x - y)$. The population density at location x and time $t + 1$, measured just after dispersal, is given by

$$n(x, t+1) = \int_{-\infty}^{\infty} k(x-y)b_n n(y, t)\,\mathrm{d}y. \tag{A2}$$

We can model population change using a density-dependent population-projection matrix, $\mathbf{B}_n$. Its entries, $b_{n,ij}$, where $i,j \in \{1, \ldots, N\}$, model the per capita production of stage i individuals at time $t + 1$ by stage j individuals at time t (see Caswell 2001). Equation (A1) has structured analog

$$\mathbf{n}(y, t+1) = \mathbf{B}_n\mathbf{n}(y, t), \tag{A3}$$

where $\mathbf{n}(y, t)$ is the vector of stage-specific population densities at location y.

Dispersal in a structured population can be described by a matrix of dispersal kernels, $\mathbf{K}(x - y)$ (Neubert and Caswell 2000), such that each entry, $k_{ij}(x - y)$, is the probability density function for the event that an individual of class j in location y at time t contributes to class i in location x at time $t + 1$, given that it also transitions from class j to class i or produces new class i individuals. For an event without associated dispersal, the corresponding dispersal kernel is $k_{ij}(x - y) = \delta(x - y)$, where $\delta(\cdot)$ is the Dirac delta function. The structured population analog to (A2) is

$$\mathbf{n}(x, t+1) = \int_{-\infty}^{\infty} [\mathbf{K}(x-y) \circ \mathbf{B}_n]\mathbf{n}(y, t)\,\mathrm{d}y. \tag{A4}$$

Again, the open circle ($\circ$) denotes the Hadamard product.

Standard Spreading Speed

Neubert and Caswell (2000) derived the invasion speed for a species colonizing new habitat according to (A4). The validity of their results rests on the linear conjecture that wave speed of the full nonlinear model is governed by its linearization at low population densities. Weinberger (1982) and Lui (1989*a*, 1989*b*) used a similar model to describe the spread of an advantageous allele in the context of population genetics, derived the same result, and proved the linear conjecture (establishing the concept of linearly predictable wave speed; Weinberger 1982). Neubert and Caswell (2000) made four assumptions: (1) $\mathbf{B}_n$ is nonnegative and primitive; (2) $\mathbf{A} = \mathbf{B}_0$ ($\mathbf{B}_n$ at $\mathbf{n} = 0$) has a dominant eigenvalue, λ,

greater than 1; (3) $\mathbf{B}_n\mathbf{n} \leq \mathbf{An}$, elementwise, for all $\mathbf{n} > 0$; and (4) all the relevant dispersal kernels, k_{ij}, have moment-generating functions. Traveling-wave solutions to the linearized problem,

$$\mathbf{n}(x, t+1) = \int_{-\infty}^{\infty} [\mathbf{K}(x-y) \circ \mathbf{A}]\mathbf{n}(y, t)\, \mathrm{d}y, \tag{A5}$$

take the form

$$\mathbf{n}(x, t) = \mathbf{w}e^{-s(x-ct)}, \tag{A6}$$

where $x - ct$ is the spatiotemporal wave variable and $c > 0$ is wave speed in the positive x-direction (Neubert and Caswell 2000). Here, s determines the shape of the low-density wave front, and the vector $\mathbf{w}$ gives the relative abundance of stages in the wave. Solutions to (A5) of form (A6) yield

$$\begin{aligned} \mathbf{w}e^{sc} &= [\mathbf{M}(s) \circ \mathbf{A}]\mathbf{w}, \\ &= \mathbf{H}(s)\mathbf{w}, \end{aligned} \tag{A7}$$

where $\mathbf{M}(s)$ is the matrix of moment-generating functions with elements

$$m_{ij}(s) = \int_{-\infty}^{\infty} e^{sx} k_{ij}(x)\, \mathrm{d}x, \tag{A8}$$

and for some $\hat{s} > 0$ the integrals in (A8) all converge for $s \in [0, \hat{s})$.

The matrix $\mathbf{H}(s) = \mathbf{M}(s) \circ \mathbf{A}$ includes information about dispersal and demography and has an eigenvalue e^{sc} and eigenvector $\mathbf{w}$ (Neubert and Caswell 2000). To create a dispersion relation between the wave speed, c, and wave steepness, s, we can equate e^{sc} to the dominant eigenvalue of $\mathbf{H}$(s) to give

$$c(s) = \frac{1}{s} \ln(\rho_1[\mathbf{H}(s)]), \tag{A9}$$

where $\rho_1[\cdot]$ denotes the dominant eigenvalue of a matrix. We define $\Omega \equiv (0, \hat{s})$ such that $\mathbf{M}(s)$ and $1/s$—and thus $c(s)$—are defined for $s \in \Omega$.

The minimum traveling wave speed for the linear system (A5) is

$$c_{\min} = \inf_{s \in \Omega} \left[\frac{1}{s} \ln\left(\rho_1[\mathbf{H}(s)]\right) \right]. \tag{A10}$$

Results proven by Lui (1989*a*) show that the original nonlinear system (A4) has a family of traveling-wave solutions, parameterized by wave speed c, that exists for all $c \geq c_{\min}$. Thus, $c_{\min}$ is also the minimum traveling wave speed for the nonlinear system (A4).

An alternate concept for population spread, which is immediately applicable to biological invasions, is that of spreading speed, c^*. Consider a population initially introduced with nonzero density over a finite region (i.e., a compact set) and zero density elsewhere. Now take the perspective of an observer that initially starts within the region of introduction and then moves outward at a constant speed, c. If c is chosen to be larger than the spreading speed, c^*, the observer will eventually outrun the invasive spread, whereas if c is chosen to be less than c^*, the invasive spread will outpace the moving observer.

To make the definition of c^* precise, we make statements about the density of individuals the observer will measure asymptotically in time. In the first instance, when $c > c^*$, the observer will measure the density of invaders to be approaching 0 asymptotically in time. In the second instance, when $c < c^*$, the observer will measure the density of invaders to be approaching the density seen far behind the invasion front—an exponentially increasing density for the linear model (A5) and typically a positive steady state for the nonlinear model (A4). A key result found by Lui (1989*a*), based on construction of upper and lower bounding solutions to (A4) and application of a comparison theorem, is that the spreading speed equals the minimum traveling wave speed, so that

$$c^* = c_{\min}, \tag{A11}$$

where $c_{\min}$ is given by (A10). Thus, we interpret the formula in (A10) as providing the speed with which an introduced organism will spread into its new habitat.

The wave shape at which $c^* = c_{\min}$ is attained is denoted s^*. At the leading edge of the invasion, the population density decays as $e^{s^* x}$.

We highlight our use of $\inf_{s\in\Omega}$ in (A10). This notation accommodates dispersal kernels for which $c(s)\to c^*$ as $s\to\infty$. In the interest of biological clarity, we slightly abuse notation in the main text and replace $\inf_{s\in\Omega}$ with $\min_{s\in\Omega}$.

The Next-Generation Matrix and Net Reproductive Number

One method for calculating R_0 begins by decomposing the population-projection matrix, $\mathbf{A}$, into matrices of stage-specific fecundities, $\mathbf{F} = [f_{ij}]$ (with $f_{i,j}\geq 0$; also sometimes called fertilities), and survival and developmental transitions, $\mathbf{T} = [\tau_{ij}]$ (with $\tau_{ij}\in[0,1]$ and column sums $\sum_i \tau_{ij}\leq 1$), such that $\mathbf{A} = \mathbf{F} + \mathbf{T}$ (Cushing and Yicang 1994). The next-generation matrix is then

$$\mathbf{Q} = \mathbf{F} + \mathbf{FT} + \mathbf{FT}^2 + \cdots = \mathbf{F}\sum_{\kappa=0}^{\infty}\mathbf{T}^{\kappa} \tag{A12}$$

(Cushing and Yicang 1994; Caswell 2001). Defining $u_i(x,g)$ as the density of individuals born into stage i in generation g ($\in\mathbb{N}$) and collecting these into the vector $\mathbf{u}(x,g)$, the next generation of a sedentary population would be given by $\mathbf{u}(x,g+1) = \mathbf{Q}\mathbf{u}(x,g)$. The Perron-Frobenius theorem guarantees that $\rho_1[\mathbf{T}]\geq 0$ (Caswell 2001), and with the additional assumption that $\rho_1[\mathbf{T}]<1$, so that $\lim_{\kappa\to\infty}\mathbf{T}^{\kappa} = 0$ (individuals do not reproduce by selfing or live forever), we can rewrite $\sum_{\kappa=0}^{\infty}\mathbf{T}^{\kappa} = [\mathbf{I}-\mathbf{T}]^{-1}$. The next-generation matrix then has a compact formula: $\mathbf{Q} = \mathbf{F}[\mathbf{I}-\mathbf{T}]^{-1}$ (Li and Schneider 2002). R_0 is $\mathbf{Q}$'s dominant eigenvalue, $\rho_1[\mathbf{Q}]$ (Cushing and Yicang 1994; Li and Schneider 2002).

Derivation of Generational Spreading Speed

In this section, we derive an expression for generational spreading speed as a function of wave shape and use that to determine the generational spreading speed. Note that $\mathbf{u}(x,g)$ and $\mathbf{u}(x,g+1)$ are not associated with a single time step, t. In fact, transition and reproduction of any generation can continue indefinitely in a stage-structured model, and in reality the life spans of two individuals in a given generation need not overlap at all. $\mathcal{L}_{\mathrm{G}}$ does, however, iterate between discrete generations.

We define $\mathbf{H}_{\mathrm{F}}(s_{\mathrm{G}}) \equiv \mathbf{M}_{\mathrm{F}}(s_{\mathrm{G}})\circ\mathbf{F}$ and $\mathbf{H}_{T}(s_{\mathrm{G}}) \equiv \mathbf{M}_{\mathrm{T}}(s_{\mathrm{G}})\circ\mathbf{T}$, where $\mathbf{M}_{\mathrm{F}}(s_{\mathrm{G}})$ and $\mathbf{M}_{\mathrm{T}}(s_{\mathrm{G}})$ are the appropriate matrices of kernel moment-generating functions.

We start by considering the region of the generational wave-shape parameter, s_{G}, in which $\rho_1[\mathbf{H}_{\mathrm{T}}(s_{\mathrm{G}})]\in[0,1)$. This condition turns out to be important—in addition to the same conditions that determine the bounds of Ω: $s_{\mathrm{G}}>0$ and all the $m_{ij}(s_G)$s existent—for ensuring a well-defined dispersion relation for the generational traveling wave.

Assuming that the dispersal kernels are exponentially bounded, $\mathbf{M}_{\mathrm{T}}(s_{\mathrm{G}})$ exists and is continuous for some region, $s_{\mathrm{G}}\in\Omega$ (defined as in the main text for standard spreading speed). Now, by definition $m_{\mathrm{T},ij}(s_{\mathrm{G}}) = \int_{-\infty}^{\infty}k_{\mathrm{T},ij}(x)e^{s_{\mathrm{G}}x}\,\mathrm{d}x$, so we have $m_{\mathrm{T},ij}(s_{\mathrm{G}})>0$ for all i,j. Thus, because $\mathbf{T}$ is a nonnegative matrix, $\mathbf{H}_{\mathrm{T}}(s_{\mathrm{G}})$ is also nonnegative. The Perron-Frobenius theorem guarantees a real dominant eigenvalue, $\rho_1[\mathbf{H}_{\mathrm{T}}(s_{\mathrm{G}})]\geq 0$ (although the magnitude of this "dominant" eigenvalue may not be unique if $\mathbf{T}$, and therefore $\mathbf{H}_{\mathrm{T}}(s_{\mathrm{G}})$, is reducible; Caswell 2001).

By definition, $m_{\mathrm{T},ij}(0) = 1$ for all i,j, so $\mathbf{H}_{\mathrm{T}}(0) = \mathbf{T}$, and we have already assumed that $\rho_1[\mathbf{T}]<1$, so $\rho_1[\mathbf{H}_{\mathrm{T}}(0)]<1$. By assumption, the $m_{\mathrm{T},ij}(s_{\mathrm{G}})$s are continuous in Ω, and $\rho_1[\mathbf{H}_{\mathrm{T}}(s_{\mathrm{G}})]$ is continuous with respect to changes in matrix elements (Meyer 2015), so there exists a region, Ω_{T}, containing $s_{\mathrm{G}} = 0$, where $\rho_1[\mathbf{H}_{\mathrm{T}}(s_{\mathrm{G}})]<1$.

We define Ω_{G} as $\Omega\cap\Omega_{\mathrm{T}}$. This turns out to be the region of s_{G} for which the generational wave-speed function is defined. If Ω_{T} does not entirely overlap Ω, then we have $\Omega_{\mathrm{G}}\subset\Omega$, and $\Omega_{\mathrm{G}} = \Omega$ otherwise. In general, $\Omega_{\mathrm{G}}\subseteq\Omega$. Importantly, $\rho_1[\mathbf{H}_{\mathrm{T}}(s_{\mathrm{G}})]<1$ in Ω_{G}.

Note that if dispersal occurs only at the time of reproduction, the dispersal kernels associated with nonzero entries of $\mathbf{T}$ will be Dirac delta functions, with associated moment-generating functions equal to 1. In this case, $\mathbf{H}_{\mathrm{T}}(s_{\mathrm{G}})$ will simply be $\mathbf{T}$, so $\Omega_{\mathrm{G}} = \Omega$.

Now, we prove a key result in deriving a formula for generational spreading speed.

CLAIM. *Let the next-generation operator take the form of (6), where $\mathcal{L}_F$ and $\mathcal{L}_T$ are as given in (5), and consider solutions of the form* $\mathbf{u}(x,g) = \mathbf{w}_G e^{-s_G(x-c_G g)}$, *as given in (7). Then* $\mathbf{w}_G e^{s_G c_G} = \mathbf{H}_F(s_G)[\mathbf{I} - \mathbf{H}_T(s_G)]^{-1}\mathbf{w}_G$ *whenever* $s_G \in \Omega_G$.

PROOF. Substituting (7) into (6) and rearranging, we have

$$\mathbf{w}_G e^{s_G c_G} = e^{s_G \xi}\mathcal{L}_F\Big\{[\mathbf{I} + \mathcal{L}_T + \mathcal{L}_T^2 + \cdots]\{e^{-s_G\xi}\mathbf{w}_G\}\Big\}, \tag{A13}$$

where $\xi = x - c_G g$ is the wave variable. To prove that the right-hand side of (A13) is equal to the right-hand side of the above claim, we take the following steps:

1. we show, by mathematical induction, that $\mathcal{L}_T^\kappa\{e^{-s_G\xi}\mathbf{w}_G\} = e^{-s_G\xi}[\mathbf{H}_T(s_G)]^\kappa\mathbf{w}_G$ for all $\kappa = 1, 2, 3, \ldots$;
2. we show that $[\mathbf{I} + \mathcal{L}_T + \mathcal{L}_T^2 + \cdots]\{e^{-s_G\xi}\mathbf{w}_G\} = e^{-s_G\xi}[\mathbf{I} - \mathbf{H}_T(s_G)]^{-1}\mathbf{w}_G$, assuming that $s_G \in \Omega_G$;
3. we show that $e^{s_G\xi}\mathcal{L}_F\{e^{-s_G\xi}\mathbf{v}\} = \mathbf{H}_F(s_G)\mathbf{v}$ for any ξ-independent vector of size N, $\mathbf{v}$;
4. we apply the result from step 2 and choose $\mathbf{v}$ for step 3 above to give $e^{s_G\xi}\mathcal{L}_F\{[\mathbf{I} + \mathcal{L}_T + \mathcal{L}_T^2 + \cdots]\{e^{-s_G\xi}\mathbf{w}_G\}\} = \mathbf{H}_F(s_G)[\mathbf{I} - \mathbf{H}_T(s_G)]^{-1}\mathbf{w}_G$; and
5. we use (A13) to show that $\mathbf{w}_G e^{s_G c_G} = \mathbf{H}_F(s_G)[\mathbf{I} - \mathbf{H}_T(s_G)]^{-1}\mathbf{w}_G$.

Below, we provide further details regarding the steps above.

1. Starting with the first-order basis case, using $\eta = y - c_G g$, making the change of variables $\zeta = \xi - \eta$, and reversing the order of integration:

$$\begin{aligned}
\mathcal{L}_T\{e^{-s_G\xi}\mathbf{w}_G\} &= \int_{-\infty}^{\infty}[\mathbf{K}_T(\xi-\eta)\circ\mathbf{T}]e^{-s_G\eta}\mathbf{w}_G\,d\eta = e^{-s_G\xi}\int_{-\infty}^{\infty}[\mathbf{K}_T(\xi-\eta)\circ\mathbf{T}]e^{s_G(\xi-\eta)}\,d\eta\mathbf{w}_G \\
&= e^{-s_G\xi}\int_{-\infty}^{\infty}[\mathbf{K}_T(\zeta)\circ\mathbf{T}]e^{s_G\zeta}\,d\zeta\mathbf{w}_G \\
&= e^{-s_G\xi}\mathbf{H}_T(s_G)\mathbf{w}_G.
\end{aligned} \tag{A14}$$

Now, assuming that $\mathcal{L}_T^n\{e^{-s_G\xi}\mathbf{w}_G\} = e^{-s_G\xi}[\mathbf{H}_T(s_G)]^n\mathbf{w}_G$,

$$\begin{aligned}
\mathcal{L}_T^{n+1}\{e^{-s_G\xi}\mathbf{w}_G\} &= \mathcal{L}_T\Big\{\mathcal{L}_T^n\{e^{-s_G\xi}\mathbf{w}_G\}\Big\} = \mathcal{L}_T\{e^{-s_G\xi}[\mathbf{H}_T(s_G)]^n\mathbf{w}_G\} \\
&= \int_{-\infty}^{\infty}[\mathbf{K}_T(\xi-\eta)\circ\mathbf{T}]e^{-s_G\eta}[\mathbf{H}_T(s_G)]^n\mathbf{w}_G\,d\eta \\
&= e^{-s_G\xi}\int_{-\infty}^{\infty}[\mathbf{K}_T(\zeta)\circ\mathbf{T}]e^{s_G(\zeta)}\,d\zeta[\mathbf{H}_T(s_G)]^n\mathbf{w}_G \\
&= e^{-s_G\xi}[\mathbf{H}_T(s_G)]^{n+1}\mathbf{w}_G.
\end{aligned} \tag{A15}$$

By induction, we have $\mathcal{L}_T^\kappa\{e^{-s_G\xi}\mathbf{w}_G\} = e^{-s_G\xi}[\mathbf{H}_T(s_G)]^\kappa\mathbf{w}_G$ for all $\kappa = 1, 2, 3, \ldots$.

2. As a direct result of step 1 above, we have that $[\mathbf{I} + \mathcal{L}_T + \mathcal{L}_T^2 + \cdots]\{e^{-s_G\xi}\mathbf{w}_G\} = e^{-s_G\xi}[\mathbf{I} + \mathbf{H}_T(s_G) + [\mathbf{H}_T(s_G)]^2 + \cdots]\mathbf{w}_G$. In addition, assuming that $s_G \in \Omega_G$, we have $\rho_1[\mathbf{H}_T(s_G)] < 1$, which implies that $\lim_{\kappa\to\infty}[\mathbf{H}_T(s_G)]^\kappa = 0$ (Li and Schneider 2002), so that $\sum_{\kappa=0}^{\infty}[\mathbf{H}_T(s_G)]^\kappa = [\mathbf{I} - \mathbf{H}_T(s_G)]^{-1}$. Thus,

$$[I + \mathcal{L}_T + \mathcal{L}_T^2 + \cdots]\{e^{-s_G\xi}\mathbf{w}_G\} = e^{-s_G\xi}[\mathbf{I} - \mathbf{H}_T(s_G)]^{-1}\mathbf{w}_G. \tag{A16}$$

3. Now, for $\mathbf{v}$, any ξ-independent vector of size N,

$$e^{s_G\xi}\mathcal{L}_F\{e^{-s_G\xi}\mathbf{v}\} = e^{s_G\xi}\int_{-\infty}^{\infty}[\mathbf{K}_F(\xi-\eta)\circ\mathbf{F}]e^{-s_G\eta}\mathbf{v}\,d\eta = \int_{-\infty}^{\infty}[\mathbf{K}_F(\zeta)\circ\mathbf{F}]e^{s_G\zeta}\,d\zeta\mathbf{v} = \mathbf{H}_F(s_G)\mathbf{v}. \tag{A17}$$

4. We can use the result of step 2 to give

$$e^{s_G\xi}\mathcal{L}_F\left\{[\mathbf{I}+\mathcal{L}_T+\mathcal{L}_T^2+\cdots]\{e^{-s_G\xi}\mathbf{w}_G\}\right\}=e^{s_G\xi}\mathcal{L}_F\{e^{-s_G\xi}[\mathbf{I}-\mathbf{H}_T(s_G)]^{-1}\mathbf{w}_G\}, \tag{A18}$$

and, applying (A17) to the right-hand side of (A18) with $\mathbf{v}$ chosen to be $[\mathbf{I}-\mathbf{H}_T(s_G)]^{-1}\mathbf{w}_G$, we have

$$e^{s_G\xi}\mathcal{L}_F\{e^{-s_G\xi}[\mathbf{I}-\mathbf{H}_T(s_G)]^{-1}\mathbf{w}_G\}=\mathbf{H}_F(s_G)[\mathbf{I}-\mathbf{H}_T(s_G)]^{-1}\mathbf{w}_G. \tag{A19}$$

5. Combining (A18) and (A19) with (A13), we see that $\mathbf{w}_G e^{s_G c_G}=e^{s_G\xi}\mathcal{L}_F\left\{[\mathbf{I}+\mathcal{L}_T+\mathcal{L}_T^2+\cdots]\{e^{-s_G\xi}\mathbf{w}_G\}\right\}=\mathbf{H}_F(s_G)[\mathbf{I}-\mathbf{H}_T(s_G)]^{-1}\mathbf{w}_G$, giving the required result. □

Defining $\mathbf{H}_G(s_G)\equiv\mathbf{H}_F(s_G)[\mathbf{I}-\mathbf{H}_T(s_G)]^{-1}$, $\mathbf{H}_G(s_G)$ is the invasion analog of the next-generation matrix, $\mathbf{Q}$. From the above claim, $e^{s_G c_G}$ is an eigenvalue of $\mathbf{H}_G(s_G)$, and we can equate $e^{s_G c_G}$ to the dominant eigenvalue of $\mathbf{H}_G(s_G)$ to create a dispersion relation (analogous to the annual case) between c_G and s_G:

$$c_G(s_G)=\frac{1}{s_G}\ln(\rho_1[\mathbf{H}_G(s_G)]). \tag{A20}$$

Note that (A20) is defined for $s_G\in\Omega_G$ ($\subseteq\Omega$), the region where $1/s_G$ is defined, all the moment-generating functions exist, and $\rho_1[\mathbf{H}_T(s_G)]<1$.

Following the arguments of Weinberger (1982), Lui (1989*a*), and Neubert and Caswell (2000), the generational spreading speed for a population, initially of finite size and restricted to a finite region of space (i.e., with compact support), is given by

$$c_G^*=\inf_{s_G\in\Omega_G}\left[\frac{1}{s_G}\ln\left(\rho_1[\mathbf{H}_G(s_G)]\right)\right]. \tag{A21}$$

Once again, in the interest of clarity, we gloss over the case where $c_G(s_G)\to c_G^*$ as $s_G\to\infty$, slightly abusing notation and replacing $\inf_{s_G\in\Omega_G}$ from (A21) with $\min_{s_G\in\Omega_G}$ in the main text.

Simplifying Cases

If dispersal is associated solely with reproduction and dispersal patterns are consistent across reproductive stages, then we can make several simplifications. All dispersal kernels associated with nonzero entries of $\mathbf{T}$ will be Dirac delta functions with moment-generating functions that are identically one, so that $\mathbf{H}_T(s_G)=\mathbf{M}_T(s_G)\circ\mathbf{T}=\mathbf{T}$. In addition, because dispersal occurs only at reproduction and is consistent across stages, we let $m_{F,ij}(s_G)=m(s_G)\,\forall\,i,j$ associated with reproduction, so that $\mathbf{H}_F(s_G)=\mathbf{M}_F(s_G)\circ\mathbf{F}=m(s_G)\mathbf{F}$. Under the simplified conditions,

$$\begin{aligned}\mathbf{H}_G(s_G)\mathbf{v}_Q&=\mathbf{H}_F(s_G)[\mathbf{I}-\mathbf{H}_T(s_G)]^{-1}\mathbf{v}_Q=m(s_G)\mathbf{F}[\mathbf{I}-\mathbf{T}]^{-1}\mathbf{v}_Q\\&=m(s_G)\mathbf{Q}\mathbf{v}_Q=m(s_G)R_0\mathbf{v}_Q,\end{aligned} \tag{A22}$$

where $\mathbf{v}_Q$ is the right eigenvector of $\mathbf{Q}$ associated with R_0. Since multiplication by a positive scalar cannot affect the ordering of eigenvalues, $\rho_1[\mathbf{H}_G(s_G)]$ is simply $m(s_G)\,R_0$ under these conditions. From (A20), the generational spreading speed becomes

$$c_G(s_G)=\frac{1}{s_G}\ln[m(s_G)R_0]. \tag{A23}$$

This is exactly the same relationship between wave shape and speed as for unstructured populations, in which $R_0\equiv\lambda$ (Kot et al. 1996; Lutscher 2007).

Now, if newly produced individuals disperse according to a normal distribution,

$$k(x-y)=\frac{1}{\sigma\sqrt{2\pi}}\exp\left[-\frac{(x-y-\mu)^2}{2\sigma^2}\right], \tag{A24}$$

with mean μ and standard deviation σ, $m(s_G) = \exp(\mu s_G + \sigma^2 s_G^2/2)$. Solving for the minimum value of $c_G(s_G)$,

$$c_G^* = \mu + \sigma\sqrt{2\ln(R_0)}, \tag{A25}$$

we see that the generational spreading speed (14) matches the conventional spreading speed for the case of growth and normal dispersal in an unstructured population (Kot et al. 1996).

Moment-Based Approximation

Without the assumption of normal (Gaussian) dispersal, we cannot solve for a general closed-form asymptotic spreading speed. For the case of unstructured populations in which individuals disperse symmetrically, however, Lutscher (2007) derived an approximation in terms of the second and fourth moments of the dispersal kernel. Note that odd moments are 0 for symmetric distributions. Since the dispersion relation (A24) recovers the wave-shape/wave-speed relationship for unstructured populations, we can, when dispersal is symmetric and growth and spread satisfy the conditions that produced the dispersion relation (A24), apply the same approximation:

$$\tilde{c}_G^* = 2\sigma\sqrt{\frac{\ln(R_0)}{2}} + \frac{\sigma}{3}\left(\sqrt{\frac{\ln(R_0)}{2}}\right)^3\gamma, \tag{A26}$$

where σ is the standard deviation of the dispersal kernel and γ is the excess kurtosis of the dispersal kernel relative to the normal distribution, so that $\gamma = \mu_4/\sigma^4 - 3$, where μ_4 is the fourth central moment (kurtosis) of the dispersal kernel (Lutscher 2007).

Invasion Criteria

In this section, we show how knowledge of the generational spreading speed for a given integrodifference model gives us information about the standard spreading speed for the same model: the sign of the generational wave-speed function (A9) matches the sign of the standard wave-speed function (A20). While this connection may seem intuitive, the potential for mathematical difficulties exists when there is a mismatch between Ω_G, the domain of existence of the generational spreading-speed function, and Ω, the domain of existence of the standard spreading-speed function.

We show (1) that the generational wave-speed function and the standard wave-speed function have the same sign at any given wave shape for which both functions exist, (2) that the generational wave-speed function exists wherever the standard wave-speed function is less than or equal to 0, and (3) that, therefore, the sign of the generational wave-speed function matches the sign of the standard wave-speed function.

Our notation has been to use s as the argument for $c(\cdot)$ and s_G as the argument for $c_G(\cdot)$. These variables describe the "steepness" of the annual and generational waves, respectively. We now introduce a general wave-shape variable, ς, that serves as an argument for both $c(\cdot)$ and $c_G(\cdot)$.

1. Consider $\varsigma \in \Omega_G$. Ω_G is a (potentially equivalent) subset of Ω, since the existence of $c_G(\varsigma)$ relies on one condition ($\rho_1[\mathbf{H}_T(\varsigma)] < 1$) in addition to those necessary for the existence of $c(\varsigma)$. We wish to establish the relationship of $c_G(\varsigma)$ and $c(\varsigma)$ to each other and to 0. Here, we rely on theorem 3.3 from Li and Schneider (2002), which we reproduce with terminology adjusted to match our own.

THEOREM. *Suppose a standard matrix model of population dynamics, given by a sequence of nonnegative vectors* $\mathbf{n}_0$, $\mathbf{n}_1, \ldots$ *of fixed length N, satisfies* $\mathbf{n}_{t+1} = \mathbf{A}\mathbf{n}_t$, $t = 0, 1, \ldots$, *where* $\mathbf{A}$ *is an* $N \times N$ *matrix with nonnegative entries and* $\mathbf{A} = \mathbf{T} + \mathbf{F}$, *and the transition matrix* $\mathbf{T}$ *satisfies* $\rho_1(\mathbf{T}) < 1$. *Denote* $\rho_1[\mathbf{A}]$ *by* λ *and* $\rho_1[\mathbf{Q}]$, *where* $\mathbf{Q} = \mathbf{F}[\mathbf{I} - \mathbf{T}]^{-1}$, *by* R_0. *Then one of the following holds:*

$$0 \le R_0 \le \lambda < 1, \; R_0 = \lambda = 1, \; \text{or} \; 1 < R_0 \le \lambda. \tag{A27}$$

If $R_0 > 0$, *then*

$$\rho_1(\mathbf{T} + \mathbf{F}/R_0) = 1. \tag{A28}$$

We wish to apply this theorem, with $\mathbf{H}(\varsigma)$ substituted for $\mathbf{A}$. While $\mathbf{H}(\varsigma)$ is not a population-projection matrix, $\mathbf{H}(\varsigma) = \mathbf{M}(\varsigma)\mathbf{A}$ satisfies $\mathbf{v}_{\kappa+1} = \mathbf{H}(\varsigma)\mathbf{v}_\kappa$ for nonnegative length-N vectors, $\mathbf{v}_\kappa$ ($\kappa \in \mathbb{N}$), since $\mathbf{M}(\varsigma)$ is nonnegative and $m_{ij}(\varsigma) > 0$ where

$a_{ij} \neq 0$, so multiplication by $\mathbf{M}(\varsigma)$ simply scales entries of $\mathbf{A}$. In addition, since $\varsigma \in \Omega_G$ by assumption, we have that $\rho_1[\mathbf{H}_T(\varsigma)] \in [0, 1)$. Thus, applying theorem 3.3 from Li and Schneider (2002), we see that for any fixed value of ς one of the following is true:

$$0 \leq \rho_1[\mathbf{H}_G(\varsigma)] \leq \rho_1[\mathbf{H}(\varsigma)] < 1,\ \rho_1[\mathbf{H}_G(\varsigma)] = \rho_1[\mathbf{H}(\varsigma)] = 1,\ \text{or}\ 1 < \rho_1[\mathbf{H}(\varsigma)] \leq \rho_1[\mathbf{H}_G(\varsigma)]. \tag{A29}$$

Combining (A29) with wave-speed functions (A9) and (A20), $c(\varsigma) = (1/\varsigma)\ln(\rho_1[\mathbf{H}(\varsigma)])$ and $c_G(\varsigma) = (1/\varsigma)\ln(\rho_1[\mathbf{H}_G(\varsigma)])$, reveals that one of the following holds:

$$c_G(\varsigma) \leq c(\varsigma) < 0,\ c_G(\varsigma) = c(\varsigma) = 0,\ \text{or}\ 0 < c(\varsigma) \leq c_G(\varsigma). \tag{A30}$$

Thus, the sign of the generational wave speed, where it exists, matches the sign of the standard wave speed attained at the same wave shape.

2. The critical threshold at which invasion stalls is $c^* = c(s^*) = 0$. An invading population will recede, losing ground in the positive x-direction with each successive time step, when $c^* < 0$. If $\Omega_G = \Omega$, (A30) implies that the generational spreading speed, c_G^*, is enough to determine whether an invasion will proceed, as the minimum values of the generational and standard wave speed functions must fall in the same range (<0, $=0$, or >0, exclusively), although they need not occur at the same critical wave-shape values.

We would like a more general guarantee that c_G^* gives us insight into whether an invasion will proceed. Because Ω_G is potentially a proper subset of Ω, the difference between the two sets, $\Omega \backslash \Omega_G$, may be nonempty. By (A30), $c_G(\varsigma)$ gives us information about $c(\varsigma)$ for ς values in Ω_G, but $c_G(\varsigma)$ does not even exist in $\Omega \backslash \Omega_G$. We wish to avoid a scenario in which $c(\varsigma) > 0$ for $\varsigma \in \Omega_G$ but $c(\varsigma) \leq 0$ for $\varsigma \in \Omega_G$. As a result, we need to know that Ω_G will not omit a critical wave-shape value, s^*, at which $c^* \leq 0$. If this were to happen, it might admit a situation in which the signs of c_G^* and c^* differed.

To have the appropriate guarantee, we must ensure that if $c(\varsigma) \leq 0$ for any ς in Ω then we will also find $c_G^* < 0$, although not necessarily at the same ς for which $c(\varsigma) \leq 0$. That is, we must show that generational spread will not occur if annual spread will not occur. If we can show that $c_G(\varsigma)$ exists, then we can use (A30) to prove that $c_G(\varsigma) < 0$ and thus that c_G^* must also be less than 0.

Claim. *For any fixed* $\varsigma \in \Omega$,

$$c(\varsigma) \leq 0 \Rightarrow \varsigma \in \Omega_G. \tag{A31}$$

Proof. The only constraint on Ω_G, in addition to those on Ω, is that $\rho_1[\mathbf{H}_T(\varsigma)]$ must be less than 1, so that $[\mathbf{I} - \mathbf{H}_T(\varsigma)]^{-1}$ (and thereby $\mathbf{H}_G(\varsigma)$) exists. Thus, $\rho_1[\mathbf{H}_T(\varsigma)] \geq 1 \Rightarrow \varsigma \in \Omega_G$. We show here that $c(\varsigma) \leq 0 \Rightarrow \rho_1[\mathbf{H}_T(\varsigma)] < 1$, so that $\varsigma \in \Omega_G$.

By (A9), $c(\varsigma) \leq 0 \Rightarrow \rho_1[\mathbf{H}(\varsigma)] \leq 1$.

By definition, $\mathbf{H}_T(\varsigma) \leq \mathbf{H}(\varsigma)$, elementwise, and at least one element of $\mathbf{H}_T(\varsigma)$ is strictly less than the corresponding element of $\mathbf{H}(\varsigma)$, since $\mathbf{H}_F(\varsigma)$, the other summand of $\mathbf{H}(\varsigma)$, contains positive entries corresponding to reproduction. As a result, the Perron-Frobenius theorem guarantees that $\rho_1[\mathbf{H}_T(\varsigma)] < \rho_1[\mathbf{H}(\varsigma)]$.

So, $c(\varsigma) \leq 0 \Rightarrow \rho_1[\mathbf{H}_T(\varsigma)] < 1$, implying that $\mathbf{H}_G(\varsigma)$ exists, and $\varsigma \in \Omega_G$. □

3. Now, to complete our argument, we must show that the signs of c^* and c_G^* match. To do this, we show that (*a*) $c^* < 0 \Rightarrow c_G^* < 0$, (*b*) $c_G^* < 0 \Rightarrow c^* < 0$, (*c*) $c^* = 0 \Rightarrow c_G^* = 0$, (*d*) $c_G^* = 0 \Rightarrow c^* = 0$, (*e*) $c^* > 0 \Rightarrow c_G^* > 0$, and (*f*) $c_G^* > 0 \Rightarrow c^* > 0$.

a. By (A31), if $c^* < 0$, $s^* \in \Omega_G$, and $c_G(s^*) < 0$ by (A30); therefore, $c_G^* \leq c_G(s^*) < 0$.
b. By (A30), if $c_G^* < 0$, then $c(s_G^*) < 0$; therefore, $c^* \leq c(s_G^*) < 0$.
c. By (A31), if $c^* = 0$, $s^* \in \Omega_G$, and $c_G(s^*) = 0$ by (A30); therefore, $c_G^* \leq 0$. If $c_G^* < 0$, then $c^* < 0$, by (A30), but we have assumed that $c^* = 0$, so $c_G^* = 0$.
d. By (A30), if $c_G^* = 0$, then $c(s_G^*) = 0$; therefore, $c^* \leq 0$. If $c^* < 0$, then $c_G^* < 0$, by (A30), but we have assumed that $c_G^* = 0$, so $c^* = 0$.
e. If $c^* > 0$, then $c(\varsigma) > 0\ \forall \varsigma \in \Omega$. By (A30), $c_G(\varsigma) > 0\ \forall \varsigma \in \Omega_G (\subseteq \Omega)$; therefore, $c_G^* > 0$.
f. If $c_G^* > 0$, then $c_G(\varsigma) > 0\ \forall \varsigma \in \Omega_G$. By (A30), $c(\varsigma) > 0\ \forall \varsigma \in \Omega_G$). Now, assume that $s^* \notin \Omega_G$. If $c^* = c(s^*) > 0$, we have our desired result. If $c^* = c(s^*) \leq 0$, then $s^* \in \Omega_G$, and we have a contradiction; therefore, $c^* > 0$.

From a through f, we have that one of the following holds:

$$c_G^* < 0 \iff c^* < 0,\ c_G^* = 0 \iff c^* = 0,\ \text{or}\ c_G^* > 0 \iff c^* > 0. \tag{A32}$$

We can, therefore, use the sign of c_G^* to draw conclusions about the sign of c^*.

Note, from (A30), that the magnitude of the generational spreading speed will be greater than the magnitude of the standard spreading speed, since c_G^* represents an upper bound on $c(s_G^*)$—and thus c^*—when c^* is positive, and c_G^* represents the lower bound on c—and thus c^*—when c^* is negative.

Graph-Reduction Calculations

Graph reduction is a technique for computing the eigenvalues of a matrix using graphical operations that are equivalent to elimination of variables, via back substitution, in the system of linear equations represented by the matrix (de-Camino-Beck and Lewis 2007). The steps involved eliminate paths and nodes from the graph representation of the matrix, appropriately transformed (Caswell 2001; de-Camino-Beck and Lewis 2007). Graph reduction has been used previously in the context of population demography to calculate both λ (Caswell 2001) and R_0 (de-Camino-Beck and Lewis 2007). Here, we adapt the graph-reduction method of de-Camino-Beck and Lewis (2007) to calculate $R_c(s_G) = \rho_1[\mathbf{H}_G(s_G)]$.

Although equivalent calculations can be performed using symbolic algebra software (e.g., Mathematica and Maple), graph reduction yields a solution expressed in terms of fecundity loops, or pathways, facilitating insight into a given matrix model's dynamical properties (de-Camino-Beck and Lewis 2007). The same result is also achievable using algebraic techniques (Rueffler and Metz 2013).

For a given matrix, we must first produce its z-transformed graph representation by dividing each matrix coefficient, corresponding to an edge of the standard matrix graph, by the unknown eigenvalue of the matrix. We can then proceed with graph reduction according to a set of simplifying rules (Mason's rules; fig. A1; Mason 1953) applied to the z-transformed graph, which preserve the associated characteristic equation (Caswell 2001).

Solving the characteristic equation associated with the reduced z-transformed graph yields the eigenvalue(s) of the original matrix. When all of the reduced graph's loops pass through a single node, as is relevant for our purposes, the characteristic equation simplifies to

$$\sum_i L^{(i)} = 1, \tag{A33}$$

where $L^{(i)}$ is the product of coefficients on the ith loop of the reduced graph (Caswell 2001). In practice, this step corresponds to summing the coefficients for each edge passing through the final remaining node of the fully reduced graph, equating this sum to 1, and then solving for the unknown eigenvalue.

The examples below come from the main text. In each case, $m(s_G)$ represents the nonunit entry, sometimes repeated, in the relevant matrix of moment-generating functions, $\mathbf{M}(s_G)$.

The graph-reduction approach to calculating R_0 relies on the fact that $\rho_1[\mathbf{F} + \mathbf{T}R_0]$ is R_0 (de-Camino-Beck and Lewis 2007). In our case, for $s_G \in \Omega_G$, $\mathbf{H}_F(s_G)$ and $\mathbf{H}_T(s_G)$ share all relevant properties of $\mathbf{F}$ and $\mathbf{T}$, respectively ($\mathbf{H}_F(s_G)$ nonnegative, $\mathbf{H}_T(s_G)$ nonnegative, $\rho_1[\mathbf{H}_T(s_G)] < 1$; see "Derivation of Generational Spreading Speed"; de-Camino-Beck and Lewis 2007), so that $\rho_1[\mathbf{H}_F(s_G) + \mathbf{H}_T(s_G)R_c(s_G)] = R_c(s_G)$. This means that we can use graph reduction on the z-transform of the modified invasion life-cycle graph, associated with matrix $\mathbf{H}_F(s_G) + \mathbf{H}_T(s_G)R_c(s_G)$, to calculate $R_c(s_G)$. In practice, we produce the z-transformed graph by multiplying fecundity weightings, f_{ij}, in the standard life-cycle graph by $m_{F,ij}(s_G)/R_c(s_G)$ and transition weightings, τ_{ij}, by $m_{T,ij}(s_G)$.

Example Details

European Green Crab

In the northwest Atlantic, green crabs mate in the summer, immediately after females molt (Berrill 1982). Eggs are released early the following summer, the planktonic larvae settle out of the water column between late summer and early autumn, and juvenile crabs develop into adults over the following years (Berrill 1982). For a postmating, postsettling winter census, we can represent the simplified life cycle using a two-stage matrix model,

$$\mathbf{A} = \begin{bmatrix} \tau_{11} & f \\ \tau_{21} & \tau_{22} \end{bmatrix}, \tag{A34}$$

where f represents the number of juvenile recruits produced per adult per year and the transition probabilities, τ_{ij}, involve independent mortality and maturation rates (ϵ and ω, respectively). Adults survive at rate $\tau_{22} = 1 - \varepsilon$, while juveniles survive and mature into adults at rate $\tau_{21} = (1 - \varepsilon)\omega$ or survive and remain juveniles at rate $\tau_{11} = (1 - \varepsilon)(1 - \omega)$. In Maine, crabs mature at 2–3 years of age and live 5–6 years (collated in Berrill 1982). Assuming fixed, independent annual survival and maturation rates and setting expected life span to 5.5 years and expected age at maturation to 2.5 years, we can solve for $\varepsilon = 2/11$ and $\omega = 2/3$.

Pringle et al. (2011) examined changes in *C. maenas* genotype frequencies along the coast of southern Nova Scotia and New England between 2000 and 2007. In the process of fitting a spatiodemographic model to observed haplotype frequencies, they estimated a one-dimensional larval dispersal kernel as a normal distribution with a mean of $\mu = -67$ km and a standard deviation of $\sigma = 234$ km (Pringle 2011). The mean value of dispersal is negative because the direction of the prevailing current is south, against the northward direction of stalled invasion that we present as the positive x-direction. We ignore adult dispersal, assuming that adult crab movement is negligible relative to the scale of larval dispersal (Pringle 2011), so we model their dispersal with the Dirac delta function, $\delta(x - y)$. Because larval dispersal takes the normal (Gaussian) form, the common matrix of dispersal kernels is

$$\mathbf{K}(x - y) = \begin{bmatrix} \delta(x - y) & \dfrac{1}{\sigma\sqrt{2\pi}} \exp\left(\dfrac{(x - y + \mu)^2}{2\sigma^2} \right) \\ \delta(x - y) & \delta(x - y) \end{bmatrix}. \tag{A35}$$

The matrix of moment-generating functions is

$$\mathbf{M}(s_G) = \begin{bmatrix} 1 & \exp\left(\mu s_G + \dfrac{(\sigma s_G)^2}{2} \right) \\ 1 & 1 \end{bmatrix}. \tag{A36}$$

To study the spatial spread of green crabs, we use graph reduction to calculate generational invasion speed analytically, defining $m(s_G) \equiv m_{12}(s_G)$. Graph reduction applied to the z-transform of matrix $\mathbf{H}_F(s_G) + \mathbf{H}_T(s_G)R_c(s_G)$ (see "Graph-Reduction Calculations") reveals that $R_c(s_G)$, the dominant eigenvalue of $H_G(s_G)$, equals $\tau_{21}m(s_G)f/[(1 - \tau_{11})(1 - \tau_{22})]$. While we demonstrate calculation of $R_c(s_G)$ for illustration purposes, we need to know R_0 to use equation (14). Noting that $R_c(s_G) = m(s_G)R_0$ in the case of larval dispersal (see "Simplification and Approximation"), we substitute R_0 and the values for μ, σ, and τ_{ij} into (14) to find the speed of the northward invasion:

$$c_G^* = -67 + 234\sqrt{2\ln\left(\frac{33}{8}f\right)}. \tag{A37}$$

California Sea Otter

Dispersal patterns in sea otters are slightly more complicated than those in the other species we have discussed. Krkošek et al. (2007) found that the best average description of the recolonization process involved a dispersal kernel that is not exponentially bounded, describing an accelerating recolonization. The relevant dispersal kernel has no moment-generating function and is thus incompatible with our framework for calculating wave speed. Lubina and Levin (1988) present an alternative hypothesis for the apparently accelerating recolonization by sea otters: after 1972, the otter population's recolonization front proceeded from kelp forest habitat into sandy bottom habitat, where the dispersal rate likely increased. Other authors have since used a Laplace kernel (Tinker et al. 2008; Smith et al. 2009).

We assume that juvenile and adult sea otters disperse according to a Laplace kernel with a mean dispersal distance of 5.19 km—the best exponentially bounded kernel fit to dispersal-distance data by Krkošek et al. (2007). Because entries of $\mathbf{A}$ are associated with reproduction or transition exclusively, we get $\mathbf{K}_F(x - y) = \mathbf{K}_T(x - y) = \mathbf{K}(x - y)$, with

$$\mathbf{K}(x-y)=\begin{bmatrix}\delta(x-y) & \frac{1}{10.38}\exp\left(\frac{-|x-y|}{5.19}\right) & \frac{1}{10.38}\exp\left(\frac{-|x-y|}{5.19}\right)\\ \delta(x-y) & \frac{1}{10.38}\exp\left(\frac{-|x-y|}{5.19}\right) & \frac{1}{10.38}\exp\left(\frac{-|x-y|}{5.19}\right)\\ \delta(x-y) & \frac{1}{10.38}\exp\left(\frac{-|x-y|}{5.19}\right) & \frac{1}{10.38}\exp\left(\frac{-|x-y|}{5.19}\right)\end{bmatrix}. \tag{A38}$$

Since $\mathbf{H}_T(s_G)$ is a triangular matrix, $\rho_1[\mathbf{H}_T(s_G)]$ is simply its largest main-diagonal element, $0.9[1-(5.19s_G)^2]^{-1}$. Solving $\rho_1[\mathbf{H}_T(s_G)]<1$ analytically, we get $0.9<1-(5.19s_G)^2 \Rightarrow s_G<0.1^{1/2}/5.19$.

To account for south-biased dispersal, we replaced the juvenile and adult dispersal kernels in (A38) with a biased Laplace kernel:

$$k_2(x-y)=\begin{cases}\frac{1}{\alpha_1-\alpha_2}\exp\left(\frac{(x-y)}{\alpha_1}\right) & \text{when } (x-y)<0,\\ \frac{1}{\alpha_1-\alpha_2}\exp\left(\frac{(x-y)}{\alpha_2}\right) & \text{when } (x-y)\geq 0,\end{cases} \tag{A39}$$

where $\alpha_{1,2}=[\upsilon\pm(\upsilon^2+\psi)^{1/2}]^{-1}$, with υ and ψ derived from a model of dispersal in a current in which individuals spread out and settle in new habitat (Lutscher et al. 2005). The ratio of the settling rate to a diffusion constant gives ψ, and the ratio of drift speed to twice the diffusion constant gives υ. To make kernel (A39) match (A38) in the absence of drift, we fix $\psi=1/\alpha^2$. Assuming this model of dispersal, we consider υ as it relates to southerly dispersal tendencies, ϑ, defined as the proportion of individuals dispersing south: $\upsilon=[\psi/([1-2\vartheta]^{-2}-1)]^{1/2}$ (Lutscher et al. 2005).

We consider φ to be the unobserved proportional change in survival rates, allowing us to consider variable survival beyond the northern recolonization boundary. Solving $R_0(\varphi)=1$ gives $\varphi\approx 0.937$; if the otter population were to experience even lower relative survival beyond the current range boundary, persistence to the north would be impossible. Thus, $\varphi<0.937$ represents the trivial case of stalled invasion, and we consider only $\varphi\geq 0.937$. We also restrict $\varphi<1/0.9$ so that individuals do not live forever and $R_0<\infty$.

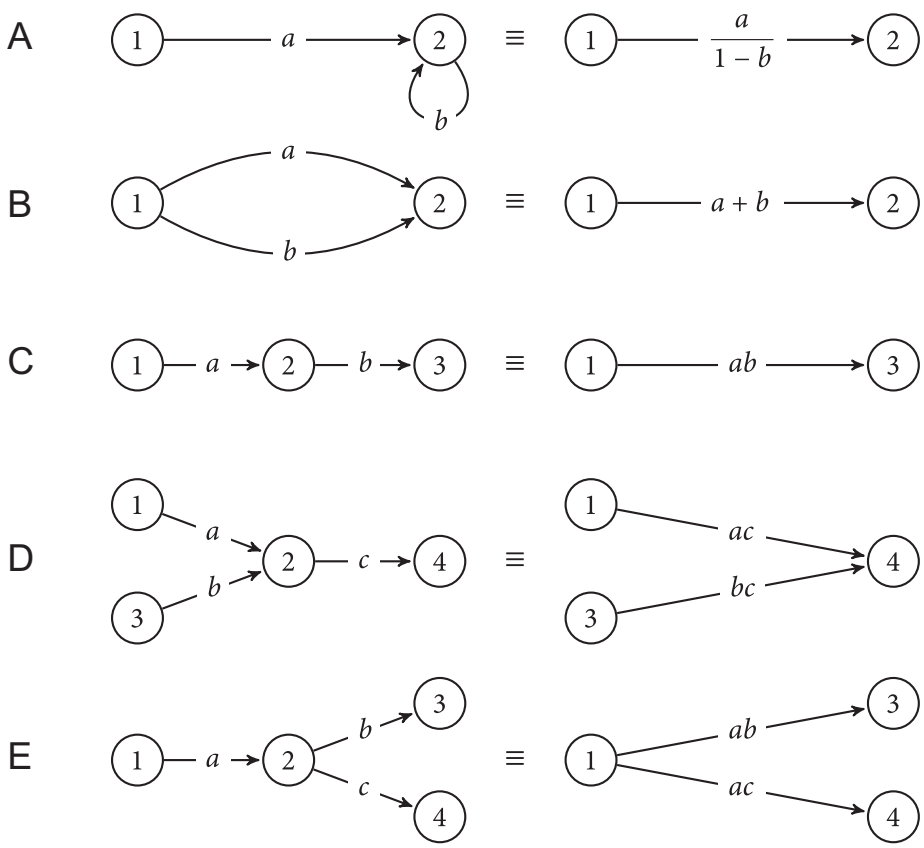

Figure A1: Mason's equivalence rules for graph reduction (modified from Caswell 2001; de-Camino-Beck and Lewis 2007). *A* shows self-loop elimination, *B* shows parallel-path elimination, and *C–E* show elimination of node 2.

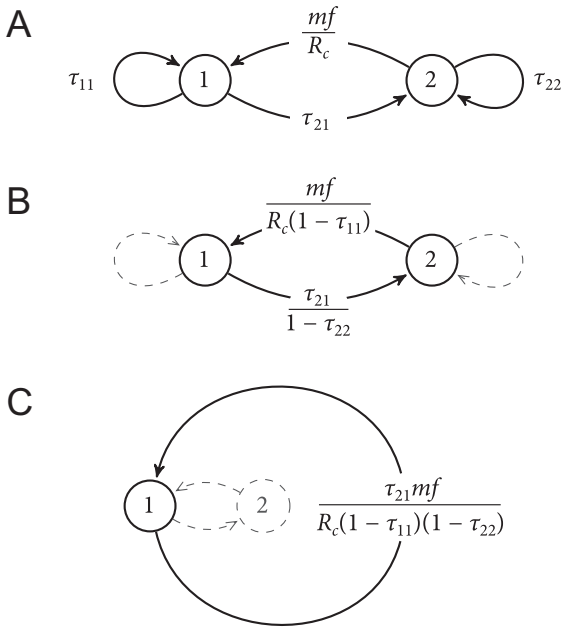

Figure A2: Graph reduction applied to the z-transformed modified invasion life-cycle graph (*A*) for the European green crab, *Carcinus maenas*. The technique is used to calculate R_c, the dominant eigenvalue of the invasion analog of the next-generation matrix (see text for details). *B* shows the elimination of self-loops, and *C* shows the elimination of node 2. The sum of self-loop weightings equals 1, so that $R_c = \tau_{21}mf/[(1-\tau_{11})(1-\tau_{22})]$. For convenience, we have omitted dependence of m and R_c on the invasion wave's shape parameter.

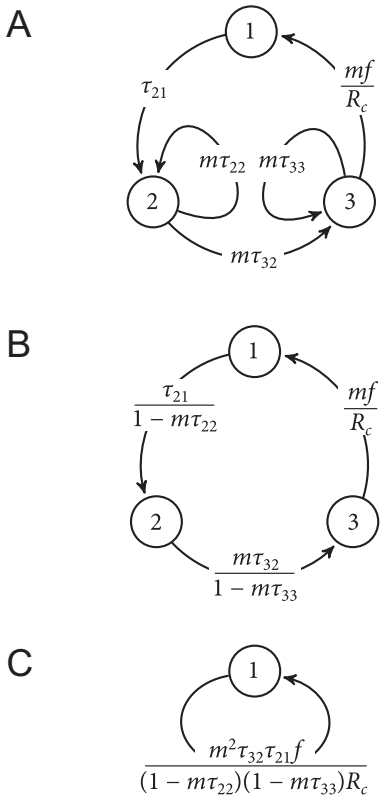

Figure A3: Graph reduction applied to the z-transformed modified invasion life-cycle graph (*A*) for the California sea otter, *Enhydra lutris nereis*. The technique is used to calculate R_c, the dominant eigenvalue of the invasion analog of the next-generation matrix (see text for details). *B* and *C* show graph-reduction steps performed according to Mason's rules (Mason 1953). The sum of self-loop weightings equals 1, so that $R_c = m^2\tau_{32}\tau_{21}f/[(1-m\tau_{22})(1-m\tau_{33})]$. For convenience, we have omitted dependence of m and R_c on the invasion wave's shape parameter.

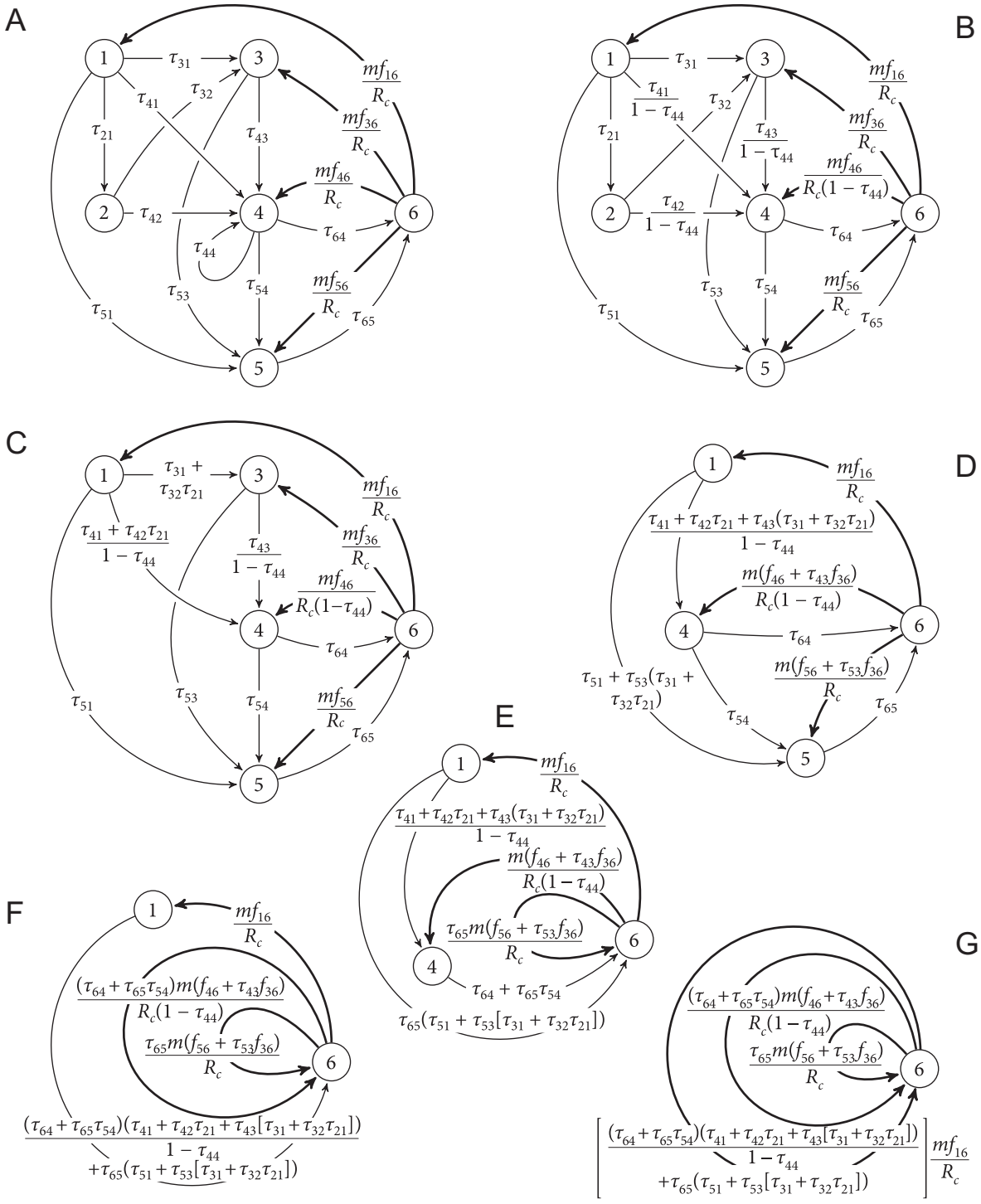

Figure A4: Graph reduction applied to the z-transformed modified invasion life-cycle graph for teasel, *Dipsacus fullonum*. The technique is used to calculate R_c, the dominant eigenvalue of the invasion analog of the next-generation matrix (see text for details). *A–G* show graph-reduction steps performed according to Mason's rules (Mason 1953). The sum of self-loop weightings equals 1, so that $R_c = ((\tau_{64} + \tau_{65}\tau_{54})[\tau_{41} + \tau_{42}\tau_{21} + \tau_{43}(\tau_{31} + \tau_{32}\tau_{21})]/(1 - \tau_{44}) + \tau_{65}[\tau_{51} + \tau_{53}(\tau_{31} + \tau_{32}\tau_{21})])mf_{16} + ((\tau_{64} + \tau_{65}\tau_{54})\tau_{43}/(1 - \tau_{44}) + \tau_{65}\tau_{53})mf_{36} + (\tau_{64} + \tau_{65}\tau_{54})/(1 - \tau_{44})mf_{46} + \tau_{65}mf_{56}$ after slight rearrangement. For convenience, we have omitted dependence of m and R_c on the invasion wave's shape parameter.